Na₃NH₂B₁₂H₁₂ as high performance solid electrolyte for all-solid-state Na-ion batteries

Liqing He[a], Huaijun Lin[b], Hai-Feng Li[c], Yaroslav Filinchuk[d], Junjun Zhang[a], Ying Liu[a], Mingyang Yang[a], Yan Hou[a], Yonghong Deng[a,**], Hai-Wen Li[e], Huaiyu Shao[c,***], Liping Wang[f], Zhouguang Lu[a,*]

[a] Department of Materials Science and Engineering, Southern University of Science and Technology, Shenzhen 518055, China
[b] Institute of Advanced Wear & Corrosion Resistance and Functional Materials, Jinan University, Guangzhou 510632, China
[c] Institute of Applied Physics and Materials Engineering (IAPME), University of Macau, Macau, China
[d] Institute of Condensed Matter and Nanosciences, Université Catholique de Louvain, Louvain-la-Neuve 1348, Belgium
[e] Kyushu University Platform of Inter/Transdisciplinary Energy Research (Q-PIT), Kyushu University, Fukuoka 819-0395, Japan
[f] State Key Laboratory of Electronic Thin Films and Integrated Devices, University of Electronic Science and Technology of China, Chengdu 610054, China

HIGHLIGHTS

- Na₃NH₂B₁₂H₁₂ with $Pna2_1$ space group is prepared for the first time.
- Outstanding electrochemical and thermal stabilities up to 10 V and 593 K.
- A high Na⁺ conductivity of $1.0 \times 10^{-4}\,\mathrm{S\,cm^{-1}}$ at 372 K.
- All-solid-state Na-ion battery repeatedly works over 200 cycles.

ARTICLE INFO

ABSTRACT

Solid electrolyte with stable and fast Na⁺ ionic conductivity is of central importance in the development of all-solid-state sodium batteries. Here we present a novel Na⁺ conductor based on complex hydrides with composition of Na₃NH₂B₁₂H₁₂. It exhibits remarkable thermal stability up to 593 K and excellent electrochemical stable window up to 10 V (vs. Na⁺/Na). It demonstrates a high Na⁺ conductivity of $1.0 \times 10^{-4}\,\mathrm{S\,cm^{-1}}$ at a temperature of 372 K, which is much higher than those of its precursors NaNH₂ and Na₂B₁₂H₁₂. All-solid-state Na-ion batteries were constructed by employing the obtained Na₃NH₂B₁₂H₁₂ as electrolyte, TiS₂ as cathode and sodium foil as anode, which can reversibly discharge/charge for over 200 cycles with more than 50% capacity retention at temperature of 353 K and a rate of 0.1 C. This work opens the gate to develop advanced solid electrolytes via combination of metal amides with closo borates.

1. Introduction

The tough issues of Li-ion batteries such as high cost and low security seem hardly to be overcome for the case of low abundance of metal Li in the earth's crust and the adoption of flammable liquid organic electrolytes. For the realization of low-carbon society in the future, development of inexpensive and safe next generation battery is urgently in great necessity. All-solid-state Na-ion battery is then proposed as one of the most competitive alternatives to Li-ion battery for: on one hand, the weight abundance of Na in the earth's crust is over 400

times more than that of Li which results in much lower cost of Na than that of Li [1,2]; on the other hand, substituting inflammable solid electrolytes for flammable liquid electrolytes remarkably increases the security of batteries during practical operation [3]. Additionally, Na is the second lightest metal element (Be is not considered for its toxicity) with similar chemical properties to Li which facilitates to high energy capacity and good compatibility to Li-ion battery devices [2].

To develop all-solid-state Na-ion battery with high performance, long cycle life and high security for commercial application, solid electrolyte materials are essential and worthy of careful study. Na-ion

---

battery solid electrolyte materials can be easily divided into polymer electrolytes and inorganic electrolytes. Polymer electrolytes such as poly (ethylene oxide) (PEO) is also commonly used in Li-ion batteries, their good ductility offers the probability to make advanced super-thin battery. Nevertheless, the solid Na-ion batteries using polymer electrolytes often exhibit serious capacity fading ($< 1/3$ of first discharge) even only after ten discharge/charge cycles which severely hampers the practical application [4,5]. Among inorganic electrolytes, β-alumina as the first super ionic conductor material used in Na-S batteries exhibits high conductivity of more than $0.2\,S\,cm^{-1}$ at 573 K [6]. However, the hygroscopicity and fragility of β-alumina as well as its demand of high operating temperature confine its application as solid electrolyte only to stationary energy storage. In NASICON structure, compounds $Na_{1+x}Zr_2Si_xP_{3-x}O_{12}$ ($0 < x < 3$) were firstly proposed as solid electrolyte materials for Na-ion battery, and a highest conductivity value of $2.7 \times 10^{-3}\,S\,cm^{-1}$ at room temperature has been achieved [2,7]. High temperature of sintering is indispensable for preparing them which increases the cost and hampers their practical application. Glass-ceramic electrolytes such as cubic Na_3PS_4 and $Na_{10}SnP_2S_{12}$ have recently been reported for Na-ion battery, both of which have room temperature conductivity of over $10^{-4}\,S\,cm^{-1}$. The disadvantages of sulfides are their poor stabilities in air or during discharge/charge cycling [8,9].

In recent years, metal complex hydrides with light weight, high electrochemical stability and excellent deformation properties [10] have attracted more and more attentions to be potential solid electrolyte materials since the first superionic conduction in $LiBH_4$ was reported [11]. Subsequently, the research of superionic conductivity was extended to $[B_{10}H_{10}]^{2-}$ and $[B_{12}H_{12}]^{2-}$ compounds which are thought to be dehydrogenation intermediate of $[BH_4]^-$ compounds and more stable [12–14]. Such complex hydrides usually exhibit a typical first-order phase transition from low-temperature phase to high-temperature phase at a certain temperature accompanying with several orders of magnitude improvement in conductivity [11–14]. Nevertheless, the phase transition temperature is usually much higher than 373 K and hardly meets the practical utilization. In order to lower phase transition temperature and increase conductivity, many new electrolytes via ionic doping or modification have been reported, such as $Li_xNa_{1-x}B_{12}H_{12}$, $NaCB_{11}H_{12}$, $Na_3BH_4B_{12}H_{12}$, $NaCB_9H_{10}$ and $Na_2B_{10}H_{10}$-$Na_2B_{12}H_{12}$ [15–20]. Though the conductivities have been much improved in optimized Na-ion complex hydride electrolytes, all-solid-state Na-ion batteries using complex hydrides as electrolytes have been rarely reported for many possible factors such as large interface resistance and poor cyclability and so on [20,21]. Poor cyclability and quick capacity fading remain the main issues for all-solid-state Na-ion batteries, and the reported reversible discharge/charge cycles in all-solid-state Na-ion batteries are usually less than 200 [8,20,22,23]. Herein, $NaNH_2$ with relatively high stability and low cost is reacted with $Na_2B_{12}H_{12}$ with high stability [24] in order to synthesize a kind of new composite electrolyte material $Na_3NH_2B_{12}H_{12}$ via simple calcination at appropriate conditions. $Na_3NH_2B_{12}H_{12}$ exhibits much higher ionic conductivity than both of $Na_2B_{12}H_{12}$ and $NaNH_2$. All-solid-state $TiS_2/Na_3NH_2B_{12}H_{12}$ | $Na_3NH_2B_{12}H_{12}$ | Na battery operated at 353 K reversibly discharges/charges for over 200 cycles and keeps more than 50% of capacity retention.

2. Experimental

Commercial $B_{10}H_{14}$ (99%, Wako), $NaBH_4$ (99.99%, Aldrich) and $NaNH_2$ (99%, ThermoFisher) were all stored in glove box and used without further purification. $Na_2B_{12}H_{12}$ was synthesized according to the reported method [25]. The reactants $NaNH_2$ and $Na_2B_{12}H_{12}$ with stoichiometric molar ratio of 1:1 were firstly hand milled for 30 min in glove box with < 0.1 ppm of H_2O/O_2 concentration. Subsequently, the hand milled reactants were sealed into ($\sim 0.7\,cm^3$) stainless steel crucibles for calcination at 523 K for 3 h. All the operation procedures were

completed in glove box protect by pure Ar.

Powder X-ray diffraction (XRD) experiments were performed by a Rigaku Smartlab X-ray diffractometer with Cu-K radiation using 45 kV/200 mA as accelerating voltage/tube current. In order to avoid air exposure during the measurement, all the sample powders were firstly placed in a quartz glass plate and then sealed by Scotch tape in glove box. Raman spectra were recorded by Horiba LabRAM HR Evolution using a green laser with a wavelength of 532 nm. The thermal stability is investigated using Thermogravimetric-Differential Thermal Analysis (TG-DTA) using 100 ml/min Ar as carrier gas.

Ionic conductivities were measured with electrochemical impedance spectroscopy for the sample pressed into a pellet with a diameter of 8 mm and a thickness of approximately 1 mm. Cu foils with a thickness of 9 μm were used as electrodes, which were mechanically fixed on both sides of the pellet sample in an air-tight 2025 coin cell. Impedance plots were measured using IM6ex electrochemistry workstation (Zahner-Elektrick, German) with a frequency range from 1 MHz to 1 Hz.

Cyclic voltammetry (CV) measurements were conducted using an IM6ex electrochemistry workstation (Zahner-Elektrick, German) with a scanning rate of 10 mV/s and voltage range from $-0.5\,V$ to 10 V. The $Na_3NH_2B_{12}H_{12}$ powder was placed in an 8-mm-diameter die and uniaxially pressed at 40 MPa and then kept for 12 h. The resultant compact electrolyte pellet was sandwiched by Na and Pt electrodes and then sealed in an air-tight 2025 coin cell for CV measurement.

The battery performance was evaluated by galvanostatic discharge/charge measurements using Neware battery test system (Shengzhen, China) at 353 K with a potential range from 1.0 to 2.4 V (vs. Na^+/Na). 50 wt% of $TiS_2/Na_3NH_2B_{12}H_{12}$ powder was used as cathode ($TiS_2 = 0.3$ mg) and pressed together with electrolyte $Na_3NH_2B_{12}H_{12}$ powder under 40 MPa for 12 h in order to make a combined pellet with both cathode and electrolyte layers. The produced pellet with 8 mm diameter is then attached to Na foil and sealed into an air-tight 2025 coin cell to assemble $TiS_2/Na_3NH_2B_{12}H_{12}$ | $Na_3NH_2B_{12}H_{12}$ | Na battery for battery performance evaluations.

3. Results and discussion

3.1. Material synthesis

$Na_2B_{12}H_{12}$ is obtained via our previously reported method [25], $Na_3NH_2B_{12}H_{12}$ is then synthesized by simple calcination of commercial $NaNH_2$ with $Na_2B_{12}H_{12}$ at different conditions (below the decomposition temperatures of both reactants). The optimal reaction condition is determined as 523 K for 3 h, the XRD pattern and Raman spectrum of thus synthesized sample are shown in Fig. 1. The XRD pattern indicates the main formation of new phase different from both $NaNH_2$ and $Na_2B_{12}H_{12}$ though with small amount of $Na_2B_{12}H_{12}$ retention ($2\theta = 15.0°$) as impurity. In Raman spectrum, only vibration signals of $[B_{12}H_{12}]^{2-}$ and $[NH_2]^-$ from $Na_2B_{12}H_{12}$ and $NaNH_2$ are obviously observed which clearly proves no decomposition of reactants but the formation of new compound $Na_3NH_2B_{12}H_{12}$.

3.2. Structural analysis

Room temperature X-ray powder diffraction was measured at constant wavelength $\lambda = 1.54184\,Å$ with a 2θ step size 0.013°. The data was refined with the FULLPROF suite [26] using the Rietveld method as shown in Fig. 2(a). An initial approximate structural model, as a starting point, was taken from the isostructural $Na_3BH_4B_{12}H_{12}$ [18]. The Pseudo-Voigt function was chosen to model the peak profile shape; the background contribution was determined using a linear interpolation between automatically selected data points; the scale factor, zero shift, lattice parameters, peak shape parameters, overall thermal parameters, preferred orientation as well as atomic positions were refined [27]. In the final analysis, all these parameters were refined
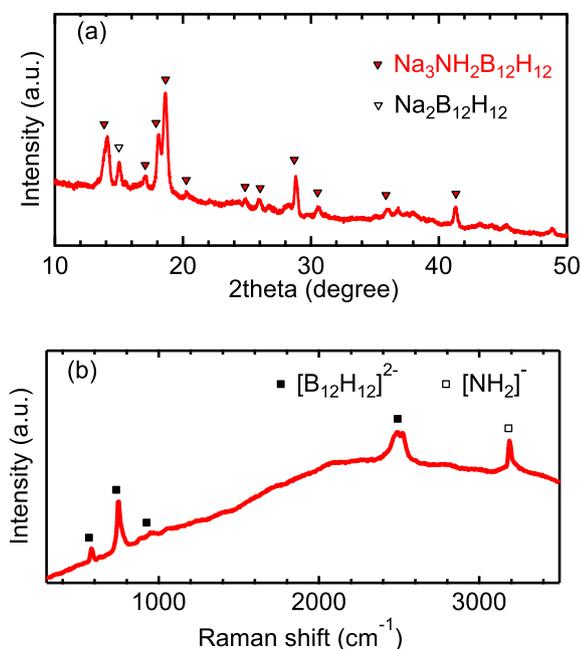
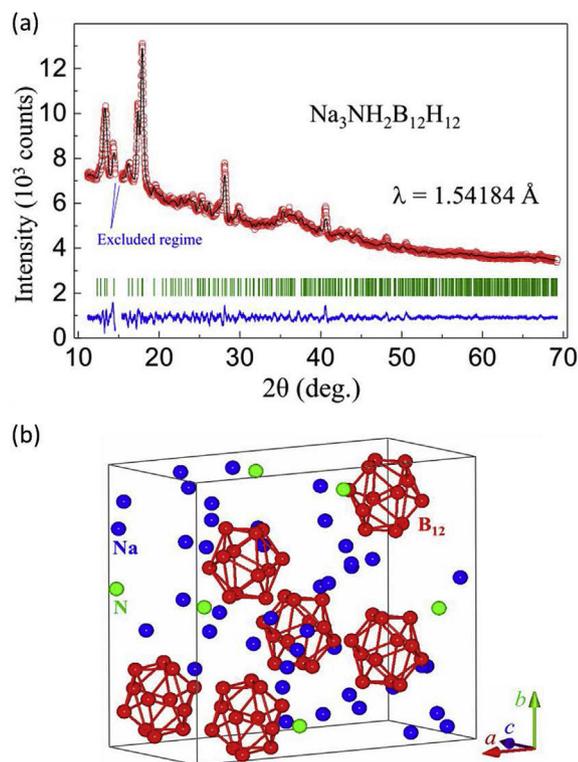**Fig. 1.** (a) XRD pattern and (b) Raman spectrum of the synthesized $Na_3NH_2B_{12}H_{12}$ (calcined at 523 K for 3 h).

Fig. 2. (a) Observed (circles) and calculated (solid lines) X-ray powder-diffraction patterns of $Na_3NH_2B_{12}H_{12}$ at ambient conditions measured with an in-house diffractometer employing the copper $K\alpha = 1.54184$ Å as the radiation. The vertical bars mark the positions of Bragg reflections. The lower curve represents the difference between the observed and calculated patterns. We excluded one regime as marked due to the presence of $Na_2B_{12}H_{12}$ impurity peak. (b) Crystal structure ($Pna2_1$) with one unit cell shown as solid lines and the building block B_{12} of $Na_3NH_2B_{12}H_{12}$. There are four B_{12} building blocks in one unit cell.

simultaneously, and the extracted results were listed in Table S1. During the refinement, the full site occupancies of all atoms were kept. To keep the building block B_{12}, the 48 B atoms were constrained in one unit cell as a whole. Since X-ray is non-sensitive to hydrogen, the intensity contribution of hydrogen atoms to the crystallographic Bragg peaks were overlooked. Fig. 2(b) shows the one crystallography unit cell of $Na_3BH_4B_{12}H_{12}$, inside which there are four B_{12} building blocks as marked. The space groups of $Na_3BH_4B_{12}H_{12}$ is noncentrosymmetric subgroups of the prototypes: $Pna2_1$ instead of $Pnam$ (a = 15.8542 (39), b = 14.3515 (24), c = 7.5327 (22) Å, V = 1713.9 (± 1.2) Å^3) at 298 K. Each atom (Na, N, B) occupies a special position with multiplicity 4. It seems that the Na conduction channel is 1D along the crystallographic c-axis.

3.3. Electrochemical and thermal stability

The electrochemical stability of $Na_3NH_2B_{12}H_{12}$ is firstly evaluated by cyclic voltammetry (CV) at room temperature using an asymmetric setup with Na and Pt as anode and cathode, respectively. The scan rate of 10 mV/s and a scan range of − 0.5–10 V are employed, as shown in Fig. S1. Cathodic and anodic currents are only observed near 0 V (vs. Na^+/Na) corresponding to sodium deposition ($Na^+ + e^- \rightarrow Na$) on the platinum electrode and sodium stripping ($Na \rightarrow Na^+ + e^-$) on Na foil, respectively. No further current due to compound decomposition up to at least 10 V (vs. Na^+/Na) is observed which indicates high electrochemical stability of $Na_3NH_2B_{12}H_{12}$ without electrochemical reactions. The CV profile shows no apparent changes except current intensity change due to material activation after 10 cycles (as shown in Fig. 3). Therefore, $Na_3NH_2B_{12}H_{12}$ with so wide potential window indicates it is a promising and suitable electrolyte material for advanced all-solid-state Na-ion battery adopting a wide range of cathodes with high voltage.

The thermal stability of $Na_3NH_2B_{12}H_{12}$ is investigated using Thermogravimetric-Differential Thermal Analysis (TG-DTA), as shown in Fig. S2. The TG curve of $Na_3NH_2B_{12}H_{12}$ showing weak weight loss (less than 1%) without DTA peaks from about 373 K similar to that in $Na_2B_{12}H_{12}$ implies the weight loss of small amount of impurities maybe from residual $B_{10}H_{14}$ (melting point at 373 K). $Na_3NH_2B_{12}H_{12}$ exhibits similar DTA peak around 473 K ascribed to the melting point of $NaNH_2$ which implies the small amount of $NaNH_2$ retention in synthesized $Na_3NH_2B_{12}H_{12}$ phase as not detected by XRD. Different from $NaNH_2$, $Na_3NH_2B_{12}H_{12}$ has higher decomposition temperature at 593 K which also suggests its application under high temperature conditions. It begins to decompose at 593 K and the decomposition product at 723 K has been collected for XRD analysis as shown in Fig. S3, the result indicates the transformation of $Na_3NH_2B_{12}H_{12}$ into $Na_2B_{12}H_{12}$ at 723 K. It is concluded that $Na_3NH_2B_{12}H_{12}$ is a suitable electrolyte at a wide temperature range from room temperature to 593 K.

3.4. Ionic conductivity

Ionic conductivity of $Na_3NH_2B_{12}H_{12}$ measured by an electrochemical impedance spectroscopy (see Fig. S4) is shown in Fig. 4. For the concerning of this material for eventually practical application, the measurement is only conducted at relatively low temperature from ~ 273 to ~ 373 K. The ionic conductivity displays a significant increase with temperature rising from 275.5 K to 372 K and reaches 1.0×10^{-4} S cm^{-1} at 372 K. Though this value is lower than recently reported $NaCB_{11}H_{12}$ [17], $Na_3BH_4B_{12}H_{12}$ [18] or $NaCB_9H_{10}$ [19], it is 3 orders of magnitude higher than that of $NaNH_2$ and 1 order of magnitude higher than that of $Na_2B_{12}H_{12}$. Besides those, it is a little higher than that of bimetallic $LiNaB_{12}H_{12}$ as reported [15]. The most important is $Na_3NH_2B_{12}H_{12}$ exhibits excellent battery cycle performance as detailedly described in the next section. All of the abovementioned content indicates that anionic doping is a very good strategy for designing advanced solid Na ionic electrolytes with higher ionic
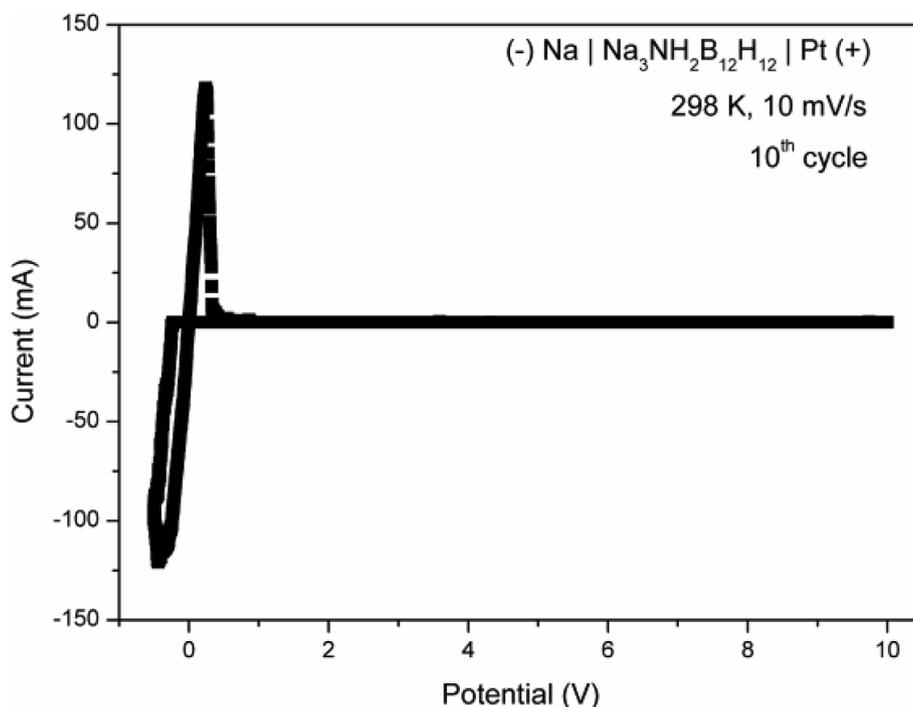
Fig. 3. Cyclic voltammogram of $Na_3NH_2B_{12}H_{12}$ sandwiched between the Na and Pt electrodes at room temperature with a voltage scan rate of 10 mV/s (10th cycle).
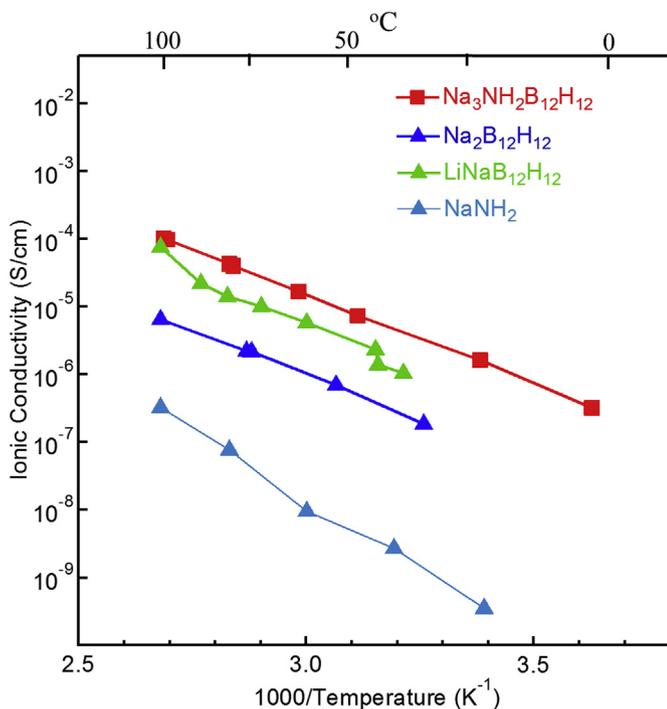

Fig. 4. Ionic conductivity measurements for $Na_3NH_2B_{12}H_{12}$ as a function of temperature. For reference, the data of the host materials $NaNH_2$, $Na_2B_{12}H_{12}$, and our previously synthesized $LiNaB_{12}H_{12}$ are also shown [15].

conductivity. The activation energy E_a for $Na_3NH_2B_{12}H_{12}$ is evaluated using the Arrhenius relationship based on Equation (1), where σ represents ionic conductivity, R is ideal gas constant and T is absolute temperature, respectively. This evaluation is completed using temperature ranging from 275.5 K to 372 K and the E_a is decided as 0.53 eV. The activation energy is hopefully further lowered by adjustment of reaction proportion of raw materials.

$$In\ \sigma = In\ \sigma_0 - \frac{Ea}{RT} \tag{1}$$

3.5. Battery performance

To further confirm the electrochemical stability and practical application of $Na_3NH_2B_{12}H_{12}$, it is mixed with active material TiS_2 in a 50:50 wt% ratio by hand milling to make a positive electrode layer. Then bulk-type, all-solid-state 50 wt% $TiS_2/Na_3NH_2B_{12}H_{12}$ | $Na_3NH_2B_{12}H_{12}$ | Na battery using $Na_3NH_2B_{12}H_{12}$ as electrolyte separator is assembled. This battery is operated repeatedly at 353 K and 0.1 C discharge and charge rates (1 C = 239 mAh g^{-1}), as shown in Fig. 5. Two voltage plateaus at ca. 2.1–2.3 V and ca. 1.2–1.7 V vs. Na/ Na^+, imply the multi-step sodium intercalation into TiS_2 with different
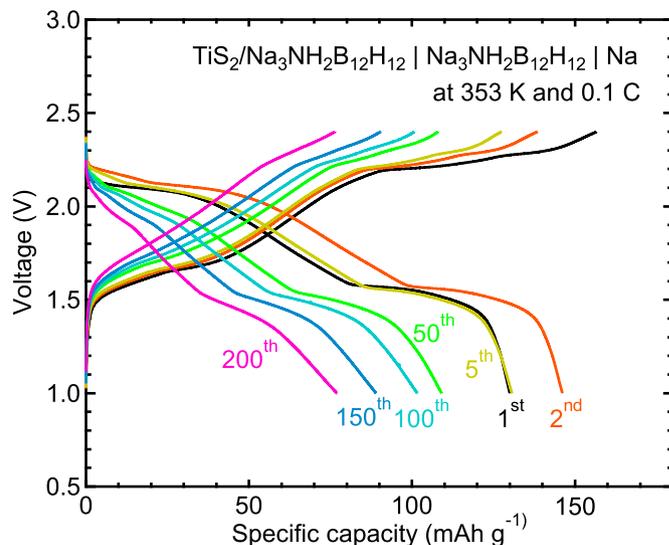

Fig. 5. Typical discharge/charge profiles over 200 cycles of all-solid-state $TiS_2/$ $Na_3NH_2B_{12}H_{12}$ | $Na_3NH_2B_{12}H_{12}$ | Na rechargeable battery operated at 353 K with a current density of 0.1 C.

Table 1
The performances of several representative all-solid-state Na-ion batteries using different materials as electrolytes.

Electrolytes	Σ (S cm^{-1})	Active materials	T_w (K)	Rates (C)	Capacities (mAh g^{-1})	Cycles
Na$_3$NH$_2$B$_{12}$H$_{12}$	1.0×10^{-4} (372 K)	TiS$_2$	353	0.1	146–77	200
Na$_2$B$_{10}$H$_{10}$-3Na$_2$B$_{12}$H$_{12}$	3.2×10^{-4} (298 K)	TiS$_2$	303	0.02	254–216	11 [20]
Na$_2$(B$_{12}$H$_{12}$)$_{0.5}$(B$_{10}$H$_{10}$)$_{0.5}$	9.0×10^{-4} (293 K)	NaCrO$_2$	333	0.05 + 0.2	80–68	250 [21]
t-Na$_{3-x}$PS$_{4-x}$Cl$_x$	1.0×10^{-3} (298 K)	TiS$_2$	298	0.1	~80	10 [29]
Na$_3$PS$_4$ glass-ceramic	1.0×10^{-4} (298 K)	TiS$_2$	298	0.01	~90	10 [8]
CPE-NZMSPO	2.4×10^{-3} (353 K)	Na$_3$V$_2$(PO$_4$)$_3$	353	0.1	~106	120 [23]

*σ = ionic conductivity; Tw = working temperature.

sodium stoichiometry in the formed Na$_x$TiS$_2$ [20]. The second discharge capacity is as high as 146 mAh g^{-1} and the battery keeps approximately 100% Coulombic efficiency (See Fig. S5) after the 2nd cycle, indicating the discharge/charge reactions occur without significant side-reactions and suggesting that Na$_3$NH$_2$B$_{12}$H$_{12}$ is a promising solid Na-ion electrolyte for practical composite electrodes. It shows a high capacity retention of 102 mAh g^{-1} after 100 cycles of discharge/charge process. What is more exciting is the battery repeatedly works over 200 cycles with capacity retention as high as 77 mAh g^{-1} which has been rarely reported in all-solid-state Na-ion battery systems, especially in those using complex hydrides as electrolytes. To re-confirm the stability of Na$_3$NH$_2$B$_{12}$H$_{12}$, the coin battery after discharge/charge 200 cycles is unpacked and the electrolyte layer is collected for XRD analysis (See Fig. S6). The results show that Na$_3$NH$_2$B$_{12}$H$_{12}$ phase still exists in large amount though with the increased proportion of Na$_2$B$_{12}$H$_{12}$ possibly coming from partial decomposition of Na$_3$NH$_2$B$_{12}$H$_{12}$. These experiments indicate Na$_3$NH$_2$B$_{12}$H$_{12}$ is a very stable and promising material as electrolyte and its decomposition during discharge/charge cycles is a very slow process. To further improve the battery performance, more work on Na$_3$NH$_2$B$_{12}$H$_{12}$ doping and modification is under way. This work opens the gate to design advanced solid electrolytes by combining metal amide with large B-H skeleton of closo borates, more advanced materials such as Na$_4$(NH$_2$)$_2$B$_{12}$H$_{12}$, Na$_3$NH$_2$B$_{10}$H$_{10}$, and Na$_2$NH$_2$CB$_9$H$_{10}$ possibly with both high stability and high ionic conductivity are hopefully to be further developed. The performances of several representative all-solid-state Na-ion batteries using different materials as electrolytes are summarized in Table 1 for a clear comparison. Generally, all-solid-state Na-ion batteries only smoothly work at small charge-discharge rates (< 1 C) because of the lower ionic conductivities of solid electrolytes than those of liquid electrolytes. Batteries working at moderate temperatures (333–353 K) usually exhibit better cycling performances than those working at room temperature. Further improvement of ionic conductivities of solid electrolytes is of great importance for retaining the better cycling performances to lower temperatures or even room temperature. The ionic conductivity of Na$_3$NH$_2$B$_{12}$H$_{12}$ is hopefully to be further improved by sodium halide (NaX) doping, reaction ratio adjustment of NaNH$_2$:Na$_2$B$_{12}$H$_{12}$ and NH$_3$ introduction for achieving solid-gas dynamic equilibrium [28]. The optimization of Na$_3$NH$_2$B$_{12}$H$_{12}$ is now under way and all-solid-state Na-ion batteries with better performances are expectable.

4. Conclusion

A new complex hydride solid-state electrolyte material Na$_3$NH$_2$B$_{12}$H$_{12}$ is successfully synthesized for the first time by simple calcination of 1:1 mol of NaNH$_2$ with Na$_2$B$_{12}$H$_{12}$. Na$_3$NH$_2$B$_{12}$H$_{12}$ with orthorhombic *Pna*2$_1$ space group exhibits outstanding electrochemical stability up to 10 V and thermal stability up to 593 K, which suggests it as a promising electrolyte material for all-solid-state Na-ion battery application. Its ionic conductivity is 3 orders and 1 order of magnitude higher than that of NaNH$_2$ and Na$_2$B$_{12}$H$_{12}$, respectively. All-solid-state battery with a structure of TiS$_2$/Na$_3$NH$_2$B$_{12}$H$_{12}$ │ Na$_3$NH$_2$B$_{12}$H$_{12}$ │ Na was constructed and operated at 353 K and 0.1 C demonstrating a

repeatedly cycling over 200 cycles with more than 50% of capacity retention, which is excellent in current all-solid-state Na-ion battery systems. This work argues that Na$_3$NH$_2$B$_{12}$H$_{12}$ analogous electrolytes are in high potential to be developed for commercial all-solid-state Na-ion battery use.

Conflicts of interest

There are no conflicts of interest to declare.

Acknowledgment

Appendix A. Supplementary data

Supplementary data related to this article can be found at http://dx.doi.org/10.1016/j.jpowsour.2018.06.054.

References

[1] D. Buchholz, A. Moretti, R. Kloepsch, S. Nowak, V. Siozios, M. Winter, S. Passerini, Chem. Mater. 25 (2013) 142–148.
[2] V. Palomares, P. Serras, I. Villaluenga, K.B. Hueso, J. Carretero-González, T. Rojo, Energy Environ. Sci. 5 (2012) 5884–5901.
[3] N. Ohta, K. Takada, L. Zhang, R. Ma, M. Osada, T. Sasaki, Adv. Mater. 18 (2006) 2226–2229.
[4] C.W. Park, H.S. Ryu, K.W. Kim, J.-H. Ahn, J.Y. Lee, H.J. Ahn, J. Power Sources 165 (2007) 450–454.
[5] J.S. Kim, H.J. Ahn, I.P. Kim, K.-W. Kim, J.H. Ahn, C.W. Park, H.S. Ryu, J. Solid State Electrochem. 12 (2008) 861–865.
[6] K.B. Hueso, M. Armand, T. Rojo, Energy Environ. Sci. 6 (2013) 734–749.
[7] R. Fuentes, F. Figueiredo, F. Marques, J. Franco, Ionics 8 (2002) 383–390.
[8] A. Hayashi, K. Noi, A. Sakuda, M. Tatsumisago, Nat. Commun. 3 (2012) 856.
[9] W.D. Richards, T. Tsujimura, L.J. Miara, Y. Wang, J.C. Kim, S.P. Ong, I. Uechi, N. Suzuki, G. Ceder, Nat. Commun. 7 (2016).
[10] K. Yoshida, A. Unemoto, H. Oguchi, S.I. Orimo, Materia 56 (2017) 448–452.
[11] M. Matsuo, Y. Nakamori, S.I. Orimo, H. Maekawa, H. Takamura, Appl. Phys. Lett. 91 (2007) 4103.
[12] M. Paskevicius, M.P. Pitt, D.H. Brown, D.A. Sheppard, S. Chumphongphan, C.E. Buckley, Phys. Chem. Chem. Phys. 15 (2013) 15825–15828.
[13] T.J. Udovic, M. Matsuo, W.S. Tang, H. Wu, V. Stavila, A.V. Soloninin, R.V. Skoryunov, O.A. Babanova, A.V. Skripov, J.J. Rush, Adv. Mater. 26 (2014) 7622–7626.
[14] T.J. Udovic, M. Matsuo, A. Unemoto, N. Verdal, V. Stavila, A.V. Skripov, J.J. Rush, H. Takamura, S.I. Orimo, Chem. Commun. 50 (2014) 3750–3752.
[15] L. He, H.W. Li, H. Nakajima, N. Tumanov, Y. Filinchuk, S.J. Hwang, M. Sharma, H. Hagemann, E. Akiba, Chem. Mater. 27 (2015) 5483–5486.
[16] W.S. Tang, T.J. Udovic, V. Stavila, J. Alloy. Comp. 645 (2015) S200–S204.
[17] W.S. Tang, A. Unemoto, W. Zhou, V. Stavila, M. Matsuo, H. Wu, S.I. Orimo, T.J. Udovic, Energy Environ. Sci. 8 (2015) 3637–3645.
[18] Y. Sadikin, M. Brighi, P. Schouwink, R. Černý, Adv. Energy Mater. 5 (2015) 1501016.
[19] W.S. Tang, M. Matsuo, H. Wu, V. Stavila, W. Zhou, A.A. Talin, A.V. Soloninin, R.V. Skoryunov, O.A. Babanova, A.V. Skripov, Adv. Energy Mater. 6 (2016)

1502237.

[20] K. Yoshida, T. Sato, A. Unemoto, M. Matsuo, T. Ikeshoji, T.J. Udovic, S.I. Orimo, Appl. Phys. Lett. 110 (2017) 103901.

[21] L. Duchêne, R.S. Kühnel, E. Stilp, E.C. Reyes, A. Remhof, H. Hagemann, C. Battaglia, Energy Environ. Sci. 10 (2017) 2609–2615.

[22] H. Pan, Y.S. Hu, L. Chen, Energy Environ. Sci. 6 (2013) 2338–2360.

[23] Z. Zhang, Q. Zhang, C. Ren, F. Luo, Q. Ma, Y.-S. Hu, Z. Zhou, H. Li, X. Huang, L. Chen, J. Mater. Chem. 4 (2016) 15823–15828.

[24] L. He, H.W. Li, E. Akiba, Energies 8 (2015) 12429–12438.

[25] L. He, H.W. Li, S.-J. Hwang, E. Akiba, J. Phys. Chem. C 118 (2014) 6084–6089.

[26] J. Rodríguez-Carvajal, Phys. B Condens. Matter 192 (1993) 55–69.

[27] H. Li, Y. Su, J. Persson, P. Meuffels, J. Walter, R. Skowronek, T. Brückel, J. Phys. Condens. Matter 19 (2007) 176226.

[28] Y.W. Tengfei Zhang, Tao Song, Hikaru Miyaoka, Keita Shinzato, Hiroki Miyaoka, Takayuki Ichikawa, Siqi Shi, Xiaogang Zhang, Shigehito Isobe, Naoyuki Hashimoto, Yoshitsugu Kojima, Joule 2 (2018) 1–12.

[29] I.H. Chu, C.S. Kompella, H. Nguyen, Z. Zhu, S. Hy, Z. Deng, Y.S. Meng, S.P. Ong, Sci. Rep. 6 (2016) 33733.